

1 **Assessment of a western blot signal for the Bcnt/Cfdp1, a tentative component of**

2 **Srcap chromatin remodeling complex; trial to overcome off-target problems**

3 Shintaro Iwashita<sup>1\*</sup>, Takehiro Suzuki<sup>2</sup>, Yoshimitsu Kiriyama<sup>1</sup>, Naoshi Dohmae<sup>2</sup>,

4 Yoshiharu Ohka<sup>1</sup>, Si-Young Song<sup>1</sup>, Kentaro Nakashima<sup>1,\*</sup>

5

6 **Affiliations:**

7 1. Kagawa School of Pharmaceutical Sciences, Tokushima Bunri University, Shido

8 1314-1, Sanuki, Kagawa 769-2193, Japan

9 2. Biomolecular Characterization Unit, RIKEN Center for Sustainable Resource

10 Science, Saitama 351-0198, Japan

11

12 \* **Corresponding authors:**

13 Shintaro Iwashita

14 E-mail: [siwast@kph.bunri-u.ac.jp](mailto:siwast@kph.bunri-u.ac.jp)

15 ORCID: 0000-0001-8086-9192

16

17 Kentaro Nakashima

18 E-mail: [nkentarokph@kph.bunri-u.ac.jp](mailto:nkentarokph@kph.bunri-u.ac.jp)

19 ORCID: 0000-0002-7881-5686

20

21 **Competing Interests: All authors declare no competing interests.**

22 **Funding: No applicable funding.**

23 **All authors approved the final version of the manuscript.**

24 **Author Contributions:**

25 Conceived, designed, performed the experiments, and wrote the manuscript: SI NK.

26 Performed mass analysis and interpretation: TS ND. Performed the experiments and

27 discussion: YK. Contributed reagents and discussion: YO. Performed the experiments

28 and wrote the manuscript: SYS.

29

## 30 **Abstract**

31           The BCNT (Bucentaur) protein family is characterized by a conserved amino  
32 acid sequence at the C-terminus (BCNT-C domain) and plays an essential role in gene  
33 expression and chromosomal maintenance in fungi, fly, and chicken. The mammalian  
34 Bucentaur/Craniofacial developmental protein 1 (Bcnt/Cfdp1) is also a tentative  
35 component of the Srcap (SNF2-Related CBP Activator Protein) chromatin remodeling  
36 complex, but little is known about its properties, partly because there are few suitable  
37 antibodies to detect the endogenous protein. We used multiple anti-Bcnt/Cfdp1  
38 antibodies against unrelated immunogens derived from BCNT-C domain and  
39 mouse-specific N-terminal peptide. To assign western blot signals and evaluate these  
40 antibodies, we utilized a stem cell line from mutant embryos of mouse *Bcnt/Cfdp1*,  
41 whose mRNA expression levels were reduced to 75% of the parental cells. In western  
42 blotting of these mutant and parental cell extracts with the anti-Bcnt/Cfdp1 antibodies,  
43 mouse Bcnt/Cfdp1 was detected as a doublet of approximately 45 kDa. LC-MS/MS  
44 analysis of the corresponding doublet for the Flag-tagged mouse Bcnt/Cfdp1  
45 constitutively expressed in T-REx 293 cell (a HEK293 derivative) exhibited that the

46 upper band was much more phosphorylated than the lower band and that there was  
47 preferential Ser phosphorylation in the WESF motif in the BCNT-C domain. Western  
48 blot with these validated antibodies indicated a preferential expression of Bcnt/Cfdp1 in  
49 the early stages of brain development in mouse and rat, which is consistent with the  
50 expression of Bcnt/Cfdp1 mRNA. This article describes the evaluation of  
51 anti-Bcnt/Cfdp1 antibodies, including a scheme to prepare a potential negative control  
52 for western blot, and discusses immune-cross reactions with off-target proteins,  
53 particularly immunoreaction probabilities.

54

## 55 **Introduction**

56 The BCNT family members in yeast, *Drosophila*, and chicken have been shown  
57 to play essential functions in gene expression and chromosomal maintenance [1].  
58 Mammalian Bcnt/Cfdp1 is also presumed to be a tentative component of the SRCAP  
59 (SNF2-Related CBP Activator Protein) chromatin remodeling complex (Human soluble  
60 protein complexes;  
61 [http://human.med.utoronto.ca/php/search\\_complex.php?clusterid=595](http://human.med.utoronto.ca/php/search_complex.php?clusterid=595)) based on the

62 analysis of Swc5, a budding yeast ortholog of Bcnt/Cfdp1, in Swr1 (yeast Sreap)  
63 chromatin complex [2-4]. Although Swc5 is not integrated with the Swr1 complex, it  
64 participates in activation of the remodeler ATPase and in the ATP-dependent histone  
65 exchange reaction, which replaces nucleosomal H2A–H2B with H2A.Z–H2B dimers by  
66 recruiting the variant H2A.Z in transcription and DNA repair [5-7]. *Swc5* is not  
67 essential for survival, but its deletion mutant *swc5Δ* cells result in genetic instability,  
68 hypersensitivity to drugs, and transcriptional misregulation because Swr1 binds to  
69 chromatin but lacks histone replacement activity [8][The *Saccharomyces* Genome  
70 Database <https://www.yeastgenome.org/>].

71 The protein structure of the Bcnt family members generally consists of an acidic  
72 N-terminal region, a highly conserved C-terminal region with about 80 amino acids  
73 (BCNT-C domain), and a hydrophilic region between them (S1 Fig and [1]). Recently,  
74 the BCNT-C domain of Swc5 was found to be essential for the histone exchange  
75 reaction [9]. On the other hand, a point mutant of the *Drosophila* ortholog, *Yeti*, which  
76 entirely lacks the BCNT-C domain, shows substantial chromosomal abnormalities,  
77 resulting in lethality before pupation [10]. Thus, the metazoan *Bcnt/Cfdp1* is essential

78 for survival in contrast to the yeast *swc5*. Furthermore, the chicken ortholog CENP-29  
79 has been identified to be a kinetochore-associated protein [11]. Given a report that  
80 CENP-B protects centromere chromatin integrity by promoting histone deposition [12],  
81 these results imply that the Bcnt members may play a broader role in the maintenance of  
82 the structure and function of the chromosome.

83 A RNA sequence analysis, as shown by the dramatic influence caused by genetic  
84 mutations of *swc5* in fission yeast [13], has revealed complex mechanisms and dynamic  
85 processes such as embryonic development and stress adaptation. However, recent  
86 studies have shown that there exists discordance between mRNA and protein expression  
87 in such dynamic processes and argue that analysis at the transcriptional level is  
88 insufficient to predict protein levels [14]. While these processes are quite complex,  
89 involving both noncoding RNAs and antisense RNAs, the western blot analysis is the  
90 most straightforward way to examine changes in target molecules at the protein level.  
91 Because the Bcnt family members may function preferentially in these dynamic  
92 processes, analysis of their protein dynamics is essential. However, most of the  
93 currently available antibodies against Bcnt/Cfdp1 are challenging to assign the correct

94 signal in western blot analysis.

95 We previously characterized human BCNT/CFDP1 (hBCNT/CFDP1) using a  
96 constitutively expressed His-tag molecule [15] and the custom-made antibody generated  
97 against an 18-mer peptide (EELAIHNRGKEGYIERKA) located in the BCNT-C  
98 domain (anti-BCNT-C Ab) [16]. Despite a calculated mass of 34.9 kDa (33.6 kDa plus  
99 His-tag) of His-hBCNT/CFDP1, the immunoreactive signal was detected around 50  
100 kDa as a doublet band on SDS-polyacrylamide gel electrophoresis (SDS/PAGE), and  
101 we showed that the difference in its apparent molecular mobility is mainly due to the  
102 acidic stretch located in the N-terminal region and Ser<sup>250</sup> phosphorylation in the  
103 BCNT-C domain [15]. However, we failed to identify the endogenous hBCNT/CFDP1  
104 due to high background caused by anti-His Ab reactive proteins and to accurately assess  
105 the specificity of the anti-BCNT-C Ab to endogenous hBCNT/CFDP1. Furthermore, we  
106 recently found that the anti-BCNT-C Ab cross-reacts with a completely unrelated target,  
107 glutamine synthetase (NP\_001035564.1; EC 6.3.1.2, which is also known as  
108  $\gamma$ -glutamyl: ammonia ligase)[17]. In this paper, we evaluate and validate the  
109 anti-Bcnt/Cfdp1 Abs and assign western blot signals using various target-related

110 materials, including *Bcnt/Cfdp1* knockdown cells. We also present a scheme to prepare  
111 a potential negative control for western blot to detect Bcnt/Cfdp1. Then, we  
112 demonstrate high expression of Bcnt/Cfdp1 at an early developmental stage of the  
113 brains of mice and rats by using the above-evaluated Abs. We also discuss off-target  
114 proteins in terms of immune reaction probability based on the analyses to solve the  
115 tasks of the present study.

116

## 117 **Results**

### 118 **Detection of Flag-tagged mBcnt as a doublet band**

119 To characterize mammalian endogenous Bcnt/Cfdp1, we first expressed  
120 Flag-tagged mouse Bcnt/Cfdp1 (F-mBcnt) in T-REx 293 cells (a derivative of HEK  
121 293) as a reference. We did this because although we previously expressed exogenous  
122 His-tagged hBCNT/CFDP1, the relatively high background by cross-reacting proteins  
123 with anti-His tag Ab made it difficult to assign the signals in western blot [15].  
124 Therefore, we used Flag-tagging to expect the lower tag specific background, though  
125 having negatively charged sequence (DYKDDDDK).



126           The mBcnt/Cfdp1 is composed of 295 amino acids, which is four amino acids less  
127 than the human counterpart. The N-terminal region has low homology between mouse  
128 and human (75%) and can be used as species-specific immunogens, while the  
129 C-terminal 82 amino acid sequence of the BCNT-C domain is identical except for two  
130 amino acid residues (S1 Fig, [1]). We isolated T-REx cell colonies that constitutively  
131 expressed F-mBcnt using G418 selection. Both the number and size of the  
132 antibiotic-resistant colonies from F-mBcnt transfectants were significantly lower and  
133 smaller than those from F-multi-cloning site (F-MCS) transfectants as a control. After  
134 growing each colony in the presence of G418, the extracts were prepared and evaluated  
135 by western blot using either anti-Flag Ab or anti-BCNT-C Ab (Fig 1, S1 Fig). Whereas  
136 all signals with anti-Flag Ab showed doublet bands, the anti-BCNT-C Ab detected one  
137 and three bands in the extracts from the F-MCS-derived and F-mBcnt derived colonies,  
138 respectively (S1 Fig). Compared with the doublet pattern between transiently expressing  
139 cells and constitutively expressing cells, the upper band (Upper) in the transient  
140 expression was significantly stronger than that of the constitutive expression (Fig 1).  
141 These features are similar to those of His-tagged hBCNT/CFDP1, as previously

142 reported [15].

143

144 **Fig 1. F-mBcnt expression as a doublet band and isolation of each band.**

145 (A) Flag-tagged mBcnt was detected as a doublet in both transient and constitutive

146 expression. The F-mBcnt or F-multi-cloning site (MCS) in the vector was expressed in

147 T-REx cells, and the extracts were prepared after culturing for 46 h as transiently

148 expressed samples (Lanes: F-MCS and F-mBcnt). In addition, the extract of the E3

149 colony that constitutively expressed F-mBcnt was prepared ( $\sim 5 \times 10^4$  cells). These

150 proteins were subjected to western blot analysis with anti-Flag Ab. The image in this

151 figure is a replica of part of S1 Fig. (B) Isolation of the upper and lower bands from

152 F-mBcnt doublet expressed in the E3 colony. The supernatant of the E3 extract isolated

153 by centrifugation was applied to anti-Flag-tag agarose beads, and the adsorbed fraction

154 was eluted, as shown in S2 Fig. After evaluation of the chromatogram, the more

155 massive Eluate #1 and #2, which had been isolated by sequential elution with Flag

156 peptide, were separated on SDA/PAGE and detected by Coomassie Brilliant Blue

157 staining. The arrows indicate a doublet band.

158

159 **Phosphorylation with serine<sup>246</sup> preference in the upper band.**

160 To reveal the molecular differences between the upper and lower bands, the bands  
161 were isolated from lysates of T-Rex-derived E3 cells that constitutively express  
162 F-mBcnt using anti-Flag Ab conjugated agarose beads (S2 Fig, Fig 1). Each band  
163 excised from the gel was digested with three different proteases—that is,  
164 *Achromobacter* protease I (API), AspN, and chymotrypsin—and each digest was  
165 subjected to LC-MS/MS analysis. In the analysis where each digested fragment covered  
166 60-67% of the entire F-mBcnt/Cfdp1 sequence, the ratios of the upper to lower bands  
167 for each fragment amounts were listed (S1 Table). Furthermore, we focused on  
168 phosphorylation sites and presented them systematically (Fig. 2). The upper band is  
169 much more phosphorylated than the lower band, and, in particular, the serine 246th  
170 mBcnt/Cfdp1 that corresponds to the S250 of hBCNT/CFDP1 is apparently the  
171 preferential site of phosphorylation. Their characteristics are very similar to those of  
172 His-tagged hBCNT/CFDP1, as previously described [15].

173

174 **Fig 2. Differential phosphorylation between the upper and lower bands of**

175 **F-mBcnt.**

176 Top panel: Molecular architecture of Flag-tagged mouse Bcnt/Cfdp1. The protein

177 shown in a large outline comprises the acidic N-terminal region, Lys/Glu/Pro-rich 40

178 amino acids (named intramolecular repeat [IR], white box), and a highly conserved

179 C-terminal region (BCNT-C domain, blue box) in addition to the Flag-tag at the

180 N-terminus (yellow box). The numbers above or below the outline show the amino acid

181 residues of the protein with (below) or without (above) the Flag tag, respectively. Three

182 black bars A, B, and C indicate the regions of focused phosphorylation sites. Each upper

183 and lower band of F-mBcnt from Fig. 1B were digested with three proteases (API,

184 AspN, and Chymotrypsin) and subjected to LC-MS/MS analysis. All of the identified

185 peptides are listed in Table S1, and their typical phosphorylated fragments and their

186 unphosphorylated counterparts are represented. Each top amino acid sequence in A, B,

187 and C represents each focused region, and the numbers at the N-terminus and the

188 C-terminus correspond to the amino acid residue of mBcnt, respectively. **Xs** are

189 different amino acid residues from human BCNT/CFDP1. Red letters show the

190 identified phosphorylated sites. Red bars indicate the ratios of the amounts of identified  
191 phosphorylated fragments in the upper band compared to those in the lower band, and  
192 blue bars show the corresponding ratios of their unphosphorylated fragments,  
193 respectively. The numbers of peptide-spectrum match (PSM) values are presented in  
194 parentheses.

195

## 196 **Evaluation of the anti-BCNT-C antibody**

197 We had assumed that the ~50-kDa signal above the F-mBcnt doublet detected by  
198 anti-BCNT-C Ab corresponds to hBCNT/CFDP1 from previous results [15]. However,  
199 the band migration was judged to be too slow on SDS/PAGE, because F-mBcnt is  
200 expected to be a slow migration due to the acid Flag tag. Therefore, we reexamined the  
201 previous data of His-hBCNT/CFDP1 [15] in the western signal by introducing  
202 anti-Bcnt/Cfdp1 Abs. We chose the two commercial anti-BCNT/CFDP1 Abs from the  
203 following criteria; the description of the immunogen is clear and the candidate signal is  
204 detected in a region significantly smaller than 50 kDa in western blot. They are  
205 26636-1-AP9 (Proteintech,

206 (<https://www.bethyl.com/product/A305-624A-M/CFDP1+Antibody>) and  
207 A305-624A-M (Bethyl,  
208 <https://www.ptglab.com/products/CFDP1-Antibody-26636-1-AP.htm>). According to  
209 each catalog, the former Ab has been generated using the larger immunogen (172-299  
210 hBCNT/CFDP1); it detects a single band with 45-50 kDa, and the specificity is  
211 validated by siRNA knockdown. The latter Ab recognizes the region of 249-299  
212 hBCNT/CFDP1, has immunoprecipitation ability and detects ~48, ~37, and ~19 kDa  
213 signals. However, we found that A305-624A-M detected only a major signal around 48  
214 kDa, whereas 26636-1-AP9 revealed other signals, including a signal of a ~50 kDa (as  
215 shown later). Based on the results, we compared western signal patterns between the  
216 anti-BCNT-C Ab and A305-624A-M using cell lysates of parent T-REx and its  
217 derivative G11 clone that constitutively expresses His-tagged hBCNT/CFDP1 [15].  
218 Both Abs efficiently recognized exogenously expressed His-hBCNT/CFDP1 in the G11  
219 extract but showed distinctly different patterns in the T-REx extract. It is noteworthy  
220 that the anti-BCNT-C Ab reacted to a band above the doublet detected with  
221 A305-624A-M (Fig 3, left panel). The difference between the two patterns was

222 confirmed by reprobing with each of the replaced Abs (Fig 3, right panel). Whereas the  
223 anti-BCNT-C Ab revealed a few other bands, A305-624A-M detected a doublet but not  
224 the bands of ~37 and ~19 kDa demonstrated in the catalog. These results strongly  
225 suggest that the distinct ~ 50-kDa band detected with anti-BCNT-C Ab as shown in S1  
226 Fig. is an off-target signal.

227

228 **Fig 3. Comparative assessment of western blot signals between the anti-BCNT-C**  
229 **antibody and A305-624A-M.**

230 The supernatants (SUPs) and their pellets (PPTs) of T-REx or its G11 cells (His-tagged  
231 human BCNT/CFDP1 constitutively expressing clone) were prepared from each cell  
232 lysate by centrifugation at 25,000 x g. Equal amounts of protein (20 µg) were subjected  
233 to western blotting analysis with either anti-BCNT-C Ab or A305-624A-M (left panel).  
234 After obtaining their images, each filter was stripped and re-probed with the exchanged  
235 Abs (right panel).

236

237 **Assigning the candidate signal of mBcnt/Cfdp1 using ES**

## 238 **mutant cells**

239 To assign the appropriate western blot signal of endogenous Bcnt/Cfdp1 and  
240 evaluate its Abs, we utilized a mouse embryonic stem (ES) cell line that is listed as  
241 homozygous *mBcnt/Cfdp1* mutant cells (i.e., double-knockout cell line) (Cfdp1-K1)[18].  
242 The gene trap vector is inserted in *mBcnt/Cfdp1* intron 5 (Fig 4A) (GenBank: accession  
243 number AG999723.1). As the BCNT-C domain is encoded by exons 6 and 7 (Fig 4A),  
244 the Cfdp1-K1 cell lysate could be used as a potential negative control for the validation  
245 of Abs generated with the BCNT-C domain as an immunogen, assuming the cells are  
246 homozygous *mBcnt/Cfdp1* mutants.

247

248 **Fig 4. Assigning western blot signals of endogenous Bcnt/Cfdp1 using mutant ES**  
249 **cells.**

250 (A) Location of the inserted gene trap vector in the Cfdp1-K1 cell. Mouse *Bcnt/Cfdp1*  
251 consists of 7 exons, and the dashed lines show their corresponding regions to  
252 Bcnt/Cfdp1. A red box indicates the gene trap vector. Two black bars under Bcnt/Cfdp1  
253 predict each location of immunogens for Ab production of anti-BCNT-C Ab (1) and



254 A305-624A-M (2), respectively. (B) RT-PCR analysis of *Bcnt/Cfdp1* mRNA from  
255 *Cfdp1*-K1 and its parental cells. Using each cDNA from *Cfdp1*-K1 (Mutant), vdR2-4  
256 (WT), or mouse brain (Cont1), RT-PCR was carried out to examine the products that  
257 correspond to (a) the full ORF of *mBcnt/Cfdp1* (928 bp) and (b) the fused region of  
258 *mBcnt* exons 1-5 and a part of *hygromycin phosphotransferase* in the gene trap vector  
259 (948 bp), respectively. The products and DNA size ladder markers were accessed by  
260 separation in agarose gel, followed by staining with ethidium bromide. (C) Assessment  
261 of western blot signal of endogenous *Bcnt/Cfdp1* using extracts of *Cfdp1*-K1 and its  
262 parental cells. Cell extracts from equal number ( $\sim 2 \times 10^5$  cells) of vdR2-4 (WT) or  
263 *Cfdp1*-K1 (Mutant) cells that had been serially passaged in the presence [Mutant (2)] or  
264 absence [Mutant (1)] of G418 and puromycin were subjected to western blot analysis  
265 with either anti-BCNT-C antibody (left filter) or 305-624A-M (right filter),  
266 respectively. A red arrow indicates a candidate signal of endogenous mouse  
267 *Bcnt/Cfdp1*.

268

269 First, we confirmed whether *Cfdp1*-K1 is knocked out on the expression of

270 *Bcnt/Cfdp1* by reverse transcription-polymerase chain reaction (RT-PCR). After  
271 subculturing in the presence or absence of G418 and puromycin, which can delete the  
272 feeder layer cells, we prepared cDNAs from Cfdp1-K1 and vdR2-4 cells; the latter is a  
273 parent cell line of Cfdp1-K1. We then examined the target *mBcnt/Cfdp1* mRNA by  
274 RT-PCR and analyzed their products by DNA sequencing. In the cDNA from  
275 Cfdp1-K1, we detected PCR products corresponding to not only the fusion gene coding  
276 *Bcnt/Cfdp1* exons 1-4 and *hygromycin phosphotransferase* derived from the gene trap  
277 vector but also the full-length *mBcnt/Cfdp1* ORF (Fig 4B). This result indicated that the  
278 gene trap vector was inserted adequately into intron 5, but Cfdp1-K1 cells were not  
279 *Bcnt/Cfdp1* double knockout. Then, a comparative transcriptome analysis by NovaSeq  
280 6000 was carried out between Cfdp1-K1 (mutant) and vdR2-4 (wild-type), and it has  
281 been shown that 694 genes were differentially expressed with a 2-fold difference, 188  
282 genes were upregulated, and 506 genes were downregulated (S1 Appendix and S2  
283 Table). Among them, *Bcnt/Cfdp1* mRNA in the Cfdp1-K1 cells was reduced to 74.4%  
284 compared to the parent cells (101.75 vs. 136.79 FPKM). Besides, the mRNAs of several  
285 housekeeping genes that are frequently used as internal controls, the flanking genes

286 *Bcar1/Cas* and *Tmem 170A*, were also significantly altered (S3 Table.).

287       Next, we examined whether anti-BCNT-C and A305-624A-M Abs detected the  
288 differential expression of Bcnt/Cfdp1 between mutant and parental cells in western blot  
289 analysis. Of the several bands detected by the anti-BCNT-C Ab, one ~45-kDa band was  
290 significantly reduced in the Cfdp1-K1 cells compared to the band intensity in vdr2-4  
291 cells by both Abs (Fig 4C). These results suggest that the ~45-kDa band is a candidate  
292 signal derived from endogenous mBcnt/Cfdp1 in mouse ES cells.

293

## 294 **Validating anti-mBcnt-N Ab and assigning the mBcnt/Cfdp1** 295 **signal**

296       As mentioned earlier, whereas the C-terminal region of BCNT members is highly  
297 conserved, the N-terminal region is variable among species. To further investigate  
298 whether the ~45-kDa band was a valid signal, we generated an anti-mBcnt/Cfdp1 Ab  
299 using a mouse-specific N-terminal peptide consisting of 16 amino acids as an  
300 immunogen (named anti-mBcnt-N Ab, Fig 5A).

301

302 **Fig 5. Validation of anti-mBcnt-N antibody.**

303 (A) Amino acid sequence alignment of the immunogen for anti-mBcnt-N Ab generation  
304 and its counterparts of rat and bovine. Mouse Bcnt/Cfdp1 is schematically shown in Fig  
305 4A. The underlined two red bars present each location of the immunogens for the  
306 generation of anti-mBcnt-N Ab and A305-624A-M, respectively. The rat and bovine  
307 counterparts are aligned, and red letters indicate the different amino acids from the  
308 immunogen peptide. (B) Equal amounts of mouse and rat brain extracts (15 or 20  $\mu\text{g}$ )  
309 and the enriched bovine placenta extract (30 or 40  $\mu\text{g}$ ) were separated on SDS/PAGE  
310 followed by western blot analyses with either anti-mBcnt-N Ab (left filter) or  
311 A305-624A-M (right filter). Each first Ab was used at a final concentration of 500  
312 ng/mL and 1  $\mu\text{g/mL}$ , respectively.

313

314 While the rat Bcnt/Cfdp1 has the same sequence as the immunogenic peptide  
315 derived from mBcnt/Cfdp1, the bovine counterpart has an entirely different amino acid  
316 sequence (Fig 5A), implying that the probability of cross-reactivity with anti-mBcnt-N  
317 Ab was expected to be very low. Indeed, we could use rat and bovine tissue extracts as

318 potential positive or negative controls, respectively, to evaluate anti-mBcnt-N Ab  
319 specificity concerning endogenous Bcnt/Cfdp1 in western blot analysis. However, since  
320 it was difficult to obtain a bovine source containing high Bcnt/Cfdp1 content, we  
321 concentrated an extract of bovine placenta with Phos-tag agarose [19], which allows  
322 enrichment of phosphorylated protein (S3 Fig), and used it for the western blot analysis  
323 (Fig 5).

324 As a result, while A305-624A-M detected a ~45-kDa signal in both tissue extracts,  
325 anti-mBcnt-N Ab detected the band in mice and rats but not in cattle. This result  
326 strongly suggests that anti-mBcnt-N Ab specifically recognizes endogenous  
327 mBcnt/Cfdp1 despite the fact that a nonspecific cross-reaction with unknown proteins  
328 was observed. We further confirmed that the ~45-kDa signal was a valid target signal  
329 using another anti-hBCNT/CFDP1 Ab, 26636-1-AP (S4 Fig). Finally, we performed  
330 western blot analysis with two Cfdp1-K1 cell lysates prepared after passage in the  
331 presence or absence of G418 / puromycin using anti-mBcnt-N Ab or A305-624A-M.  
332 The results showed that both Abs recognized a ~45-kDa band with significantly reduced  
333 intensity in both Cfdp1-K1 lysates as compared to that in the parental cell lysate (Fig 6).

334 From these results, we concluded that the ~45-kDa signal is derived from the

335 endogenous mBcnt/Cfdp1.

336

337 **Fig 6. Assignment of western blot mBcnt/Cfdp1 signals.**

338 Equal amounts of cell extract (20 µg protein) of vdR2-4 (WT) or Cfdp1-K1 (Mutant)

339 cells serially passaged in the presence [Mutant (2)] or absence [Mutant (1)] of G418 and

340 puromycin were subjected to western blot analysis with anti-mBcnt-N Ab (left panel) or

341 A305-624A-M (right filter). A red arrow indicates a signal of mouse Bcnt/Cfdp1. A

342 band detected with anti-mBcnt-N Ab at ~75 kDa (shown as \*) is probably the fusion

343 protein of a part of mBcnt (derived from exon 1-5) and hygromycin phosphotransferase.

344 It is 63.9 kDa as a calculated molecular mass but may run slowly on SDS/PAGE due to

345 the acid stretch located in the N-terminal region of the mouse Bcnt/Cfdp1.

346

347 To confirm whether the ~45-kDa band detected by the both Abs is identical, the

348 filter that had been detected with anti-mBcnt-N Ab was reprobbed with A305-624A-M.

349 The result indicated that the signal was identical.

350

351 **Expression of mBcnt/Cfdp1 in the early stage of brain**  
352 **development**

353 RNA profiling data of the mouse and rat ENCODE (The Encyclopedia of DNA  
354 Elements) projects show that Bcnt/Cfdp1 mRNA expresses ubiquitously and  
355 preferentially in the early stage of development. However, recent studies have revealed  
356 pervasive discordance between mRNA levels and protein levels, especially in  
357 embryonic development [14]. Therefore, we examined mBcnt/Cfdp1 expression in the  
358 cerebrum of mouse and rat, focusing on developmental stages using the evaluated  
359 anti-Bcnt/Cfdp1 Abs above. The results showed that mBcnt/Cfdp1 preferentially  
360 expresses in the early stages and significantly decreased according to the postnatal  
361 stages in the rat cerebrum (Fig 7).

362

363 **Fig 7. Bcnt/Cfdp1 expression of rodent brain in the early stage of development.**

364 Equal amounts (20 µg of protein) of cerebrum extracts of the embryo around 17 days  
365 (E17) and P0 mouse and rat postnatal day samples (denoted by P# on the top of each

366 lane) were loaded and subjected to western blotting analysis with anti-mBcnt-N Ab (left  
367 panel) or A305-624A-M (middle panel). The latter filter was re-probed with another  
368 anti-BCNT/CFDP1 Ab, 26636-1-AP (right panel). The filters were finally stained with  
369 Coomassie Brilliant Blue (CBB) to check the amounts of loading proteins (bottom  
370 panel).

371

## 372 **Discussion**

373 In this paper, we assigned the endogenous mBcnt/Cfdp1 signal in western blot,  
374 validated anti-mBcnt/Cfdp1Abs by utilizing various target-related materials, and  
375 showed that mouse and rat Bcnt/Cfdp1 expressed preferentially at early stages of brain  
376 development. Moreover, based on the problems encountered when attempting to solve  
377 these tasks in the present study, we discuss immune-cross reactions with off-target  
378 proteins from the viewpoint of immune reaction probability.

379 We generated F-mBcnt instead of His-tagged hBCNT/CFDP1 because the latter  
380 made it challenging to evaluate the specificity of anti-Bcnt/Cfdp1 Abs due to the  
381 difficulty to distinguish specific immune-positive signals from the high background of



382 anti-His tag positive proteins [15]. Indeed, Nono (p54<sup>rnb</sup>)[20], which contains the  
383 HHQHHH sequence in the N-terminus region, could be isolated using anti-His-tag  
384 Ab-conjugated beads (S6 Fig). F-mBcnt appeared as a doublet, and the upper band was  
385 much more phosphorylated than the lower band-in particular, the phosphorylation of the  
386 Ser<sup>246</sup> residue in the WESF motif of the BCNT-C domain was characteristic. The  
387 mBcnt/Cfdp1 doublet was probably caused by the presence or absence of Ser<sup>246</sup>  
388 phosphorylation because this characteristic phosphorylation is very similar to that of  
389 His-tagged hBCNT/CFDP1, as previously described [15]. Though its biological  
390 significance is not yet clear, one interesting possibility is that this phosphorylation  
391 might be a determinant of the intracellular localization of Bcnt/Cfdp1.

392           We first evaluated a custom-made anti-BCNT-C Ab that detected a distinct  
393 band from those detected by anti-Flag Ab in F-mBcnt-expressing cell lysates (S1 Fig).  
394 We initially assumed that the band was hBCNT/CFDP1. By introducing another  
395 commercially available anti-hBCNT/CFDP1 Ab (i.e., A305-624A-M from Betyl  
396 laboratory), we compared the immune-positive signals detected with ant-BCNT-C Ab  
397 and found that their patterns were distinctively different in the parental cell extract. On

398 the other hand, the exogenous hBCNT/CFDP1 in the extract of G11 clone were well  
399 recognized by both Abs. Therefore, we utilized a Cfdp1-K1 cell line that has been  
400 produced by a library of random mutations introduced by gene trap vector insertion in  
401 Bloom-deficient ES cells, selected for populations of homozygous mutant cells  
402 following mitotic recombination [18], and was listed as a cell line of mouse *Bcnt/Cfdp1*  
403 homozygous mutant (Japanese Collection of Research Bioresources (JCRB) Cell  
404 Bank\_AyuK7D01). However, RT-PCR analysis of cDNA from Cfdp1-K1 revealed the  
405 presence of mRNA corresponding to the full-length ORF of the *mBcnt/Cfdp1*. Indeed, a  
406 comparative analysis of transcriptome RNA sequencing between Cfdp1-K1 and its  
407 parent cells showed that *Bcnt/Cfdp1* mRNA levels were 74.4%. Splicing may efficiently  
408 occur by skipping the acceptor site in the trap gene vector, which is located in the intron  
409 5 spanning over 50 kb (Fig 4A). Although the Cfdp1-K1 cell line was not *Bcnt/Cfdp1*  
410 double knockout, it is useful as *Bcnt/Cfdp1* knockdown mutant cells to detect a strong  
411 candidate signal at ~45 kDa. On the other hand, an attempt has been made to generate  
412 dog *Bcnt/Cfdp1* knockout MDCK (Madin-Darby Canine Kidney) cells by targeting its  
413 exon 1 according to the same strategy as the production of  $\beta$ - and  $\gamma$ -catenin double-

414 knockout cells [21], but the expected cells were not obtained so far (W. Kobayashi,  
415 personal communication). Finally, we were able to assign the signal of endogenous  
416 mBcnt/Cfdp1 detected by two Abs raised against unrelated immunogens. One of the  
417 antigens is a mouse-specific N-terminal peptide, and the other is a peptide of BCNT-C  
418 domain, which is highly conserved in mammalian Bcnt/Cfdp1.

419 The following is evidences that the ~45-kDa band is the signal of endogenous  
420 Bcnt/Cfdp1 in western blot. First, among several signals detected by the anti-BCNT-C  
421 Ab, the ~45-kDa signal was significantly reduced in the western blot of the  
422 mBcnt/Cfdp1 mutant cell extract compared to the signal of the parent cell (Fig 4C).  
423 Second, the ~45-kDa signal was detected by two other antibodies (i.e., anti-mBcnt-N  
424 Ab and A305-624A-M), each of which was generated using mutually unrelated  
425 immunogens (Fig 6) as well as another anti-hBCNT/CFDP1 Ab, 26636-1-AP (S4 Fig).  
426 We confirmed the specificity of the anti-mBcnt-N Ab concerning the ~45-kDa signal by  
427 preparing enriched bovine Bcnt/Cfdp1 with Phos-tag agarose (Fig 5) as a potential  
428 negative control in a western blot.

429           The target band at ~45-kDa appears significantly smaller than signals reported by  
430 many available anti-Bcnt/Cfdp1 Abs, including our custom-made anti-BCNT-C Ab.  
431 The molecular behavior of ~50-kDa protein reported with many anti-hBCNT/CFDP1  
432 Abs was significantly different from that of endogenous Bcnt/Cfdp1 (S1 Fig and Figs 3  
433 and 4C); therefore, the 50-kDa signal is probably a common non-specific band(s). Since  
434 we used this anti-BCNT-C Ab, our initial conjectures regarding the 50-kDa signal (refer  
435 to abstract in [15]), the 43-kDa signal (glutamine synthetase, [17]) (refer to Fig 3C in  
436 [16] and Fig 1B in [22]) determined by western blot analysis, and the intracellular  
437 localization by immunostaining (refer to Fig 6b in [23]) were all misdirected. On the other  
438 hand, we did not recognize two bands at ~37 and ~19 kDa, which are shown in the  
439 catalog of A305-624A-M. Furthermore, although five isoforms of *mBcnt/Cfdp1* have  
440 been reported (*Mus musculus*, NCBI Accession No. ID: 23837), we could not identify  
441 any isoforms during our western blot analyses.

442           It was evident that the anti-BCNT-C Ab detected a weak signal to the target  
443 molecule (Fig 4C). A similarly difficult situation must occur with many Abs, which is  
444 considered to be problematic (e.g., [24], [25]). Concerning the time-consuming

445 validation of anti-Bcnt/Cfdp1 Ab using western blot, we consider the intrinsic issues  
446 that may have led to its inappropriate assignment and how these could be resolved.  
447 First, we should use the information of preferential expression of Bcnt/Cfdp1  
448 mRNA—for example, mouse embryo brain is more suitable than the adult brain as  
449 screening samples for its Ab evaluation. Second, although we needed other independent  
450 anti-BCNT-C Abs and attempted to prepare them using the N-terminal region as  
451 immunogens, we failed to obtain the appropriate Abs that could be utilized at that time.  
452 Third, although non-specific band patterns detected by Abs raised against different  
453 immunogens are generally not identical, many available anti-Bcnt/Cfdp1 Abs including  
454 the anti-BCNT-C Ab and 26636-1-AP, commonly detected a relatively strong signal(s)  
455 near 50-kDa, and thus resulted in an incorrect assignment. Regarding the second and  
456 third points, the properties of Bcnt/Cfdp1 may be related since it mainly consists of  
457 structurally disordered regions. It is noteworthy that the epitopes from disordered  
458 antigens are smaller than those from the ordered counterparts and that they interact  
459 more efficiently with their Abs [26]. Thus, the anti-Bcnt/Cfdp1 Abs generated against  
460 most parts of the molecule as immunogens may cause cross-reaction with various

461 proteins with high affinity, resulting in the poor quality of antisera. Fourth, complex  
462 migration of Bcnt/Cfdp1 on SDS/PAGE made it challenging to assign a valid signal.  
463 BCNT/CFDP1 as well as mBcnt/Cfdp1 is expressed as a doublet band and migrates  
464 slower on SDS/PAGE than expected from the calculated molecular mass (33.6 kDa of  
465 human BCNT/CFDP1 and 32.7 kDa of mouse Bcnt/Cfdp1). This feature may be mainly  
466 due to the acid stretch of the N-terminal region and the Ser phosphorylation of the  
467 BCNT-C domain [15]. Lastly, despite a lack of substantial evidence that *Bcnt/Cfdp1* is  
468 directly involved in craniofacial development, its attractive but misleading  
469 nomenclature (i.e., craniofacial development protein 1) may have caused confusion  
470 regarding its function in Ab providers and researchers. As a result, this may have  
471 prevented prior careful analysis of the molecule.

472 Off-target problems have been widely discussed in many Ab validation studies  
473 (e.g., [24], [25]), including specific in-depth efforts for Ab evaluation (e.g., [27]).  
474 Moreover, a strategy for Ab validation has been proposed [28]. However, the focus of  
475 this discussion appears to be blurred, at least regarding western blot analysis.

476 Immune cross-reactivity of Abs is based on a general chemical reaction determined  
477 by the reaction probability. Epitopes are conventionally divided into two categories:  
478 linear or sequential and discontinuous or conformational epitopes [29]. However, Abs  
479 do not recognize even linear epitopes as a series of amino acid residues but rather the  
480 physicochemical and stereochemical states that they constitute, and these properties as a  
481 whole constitute epitope [30, 31]. For example, the following two cases may reflect  
482 topological or stereochemical similarity of small environments that determine the  
483 common epitopes between completely different proteins: Bcnt/Cfdp1 and glutamine  
484 synthetase [17] and phosphocasein and  $\beta$ -actin [32], respectively. Thus, in principle, it is  
485 impossible to exactly match the properties of the epitope with their amino acid  
486 sequences, even in linear epitopes. Furthermore, it has been shown that linear epitope  
487 peptides that reveal apparent off-target binding at the peptide levels have a strict  
488 conformational component at the protein levels [33]. The classification of two types of  
489 epitopes is therefore not easily producible.

490 Western blot signals detected by a certain Ab are strongly influenced by the target  
491 concentration in test samples, as shown in Fig 3. The anti-BCNT-C Ab recognized the

492 exogenously expressed His-tag hBCNT/CFDP1 but scarcely detected an endogenous  
493 counterpart. The result implies that the extract of cells overexpressing a target protein  
494 does not qualify as a positive control for Ab evaluation in some experiments. However,  
495 a good Ab means that it is useful to reveal new evidence regardless of the type of  
496 experiment, which depends mainly on the target concentration to be analyzed and the  
497 extract preparation method (Figs 3 and 5 and [25]). The experimental materials are quite  
498 different with respect to their species, tissues, and developmental stages. Besides, when  
499 the target gene has a strong influence on other genes or when the target is a lowly  
500 expressed protein, some efforts may be required to assign their appropriate target  
501 signals even using lysates from knockout or knockdown cells as a negative control. As  
502 shown by the effect of Bcnt/Cfdp1 knockdown in Cfdp1-K1 cells, it is not uncommon  
503 that a single gene mutation dramatically alters the expression levels of other genes (S3  
504 Table and S4 Table). Furthermore, it is possible that many proteins showing similar  
505 mobility with the target molecule on SDS/PAGE overlap the migration region of the  
506 target molecule, making the signal assignment challenging [34]. There is no guarantee  
507 that the once validated Ab will work with other samples.



508           Of course, what we can do is generate antibodies using many unrelated  
509 immunogens and also eliminate troublesome off-targets by rigorously screening  
510 candidate antibodies (e.g., [28]). However, it is not necessary to be concerned with a  
511 single signal, and even if a few off-target signals are detected, these kinds of Abs can be  
512 useful if we have evaluated their limitation correctly, as shown in Fig 5 and in many  
513 reports (e.g., [35]). Abs do not act within the confines of all-or-nothing modes via  
514 specific reactions; therefore, it is critical to understand the efficacy and limitations of  
515 the antibody used in any experiments.

516           Although sensitivity of western blot analysis to crude extract is much better than  
517 that of mass spectroscopy, these tools are fundamentally different—that is, individual Ab  
518 is not a tool for identifying a molecule but rather a tool for checking a contradiction.  
519 Recently, mass analyses have become remarkably advanced and widely available. Thus,  
520 it is now much easier to identify molecules that have been considered to be false targets  
521 due to wrong-cross reaction with Abs. These trials may provide byproducts of the  
522 excellent Abs, such as conformation-specific antibodies against the proteins.

523           As a reliable anti-Bcnt/Cfdp1 Ab (i.e., A305-624A-M) becomes clearer at present, it  
524 is possible to characterize endogenous Bcnt/Cfdp1 more accurately, including  
525 subcellular fractionation and tissue distribution. On the other hand, the comparative

526 transcriptome analysis of Cfdp1-K1 cells revealed that only a 25% decrease in  
527 Bcnt/Cfdp1 mRNA resulted in a marked up-regulation or down-regulation of many  
528 genes (S1 Appendix, S2 Table), though the confirmation is required by generating their  
529 revertant cells by removing the mutagenic vector sequences through Flp-FRT  
530 recombination [18]. Among them, it is noteworthy that mRNA expression of  
531 intermediate filaments of keratins 8, as well as 18 and 19, was dramatically suppressed  
532 –that is, 1% relative to the parental cells (S4 Table, [36]). Given the function of Swc5,  
533 which is required under stressed conditions and conditions requiring rapid transcription  
534 ([*Saccharomyces* Data Base], [6], and [7]), Bcnt/Cfdp1 may play an essential role for  
535 maintaining cell homeostasis, especially in processes such as developmental stage, cell  
536 differentiation, and DNA damage repair. The Cfdp1-K1 cell line may serve as a stable  
537 Bcnt/Cfdp1 knockdown cell in elucidating the functional role of Bcnt/Cfdp1 in the early  
538 developmental stage by using western blotting analysis with further reliable  
539 anti-Bcnt/Cfdp1 Abs.

540

## 541 **Materials and Methods**

542 All of the reagents and materials, and primers used are listed as S5 Table and S6 Table,  
543 respectively.

## 544 **Ethical approval**

545 All of the genetic recombination experiments and all of the animal experiments  
546 in the present study were approved by the Genetic Recombination Experiment Safety  
547 Committee and the Animal Care and Use Committee, respectively, of Tokushima Bunri  
548 University. All of the experiments were performed in accordance with NIH Guidelines  
549 for the Care and Use of Laboratory Animals.

550

## 551 **Cell culture**

552 T-REx-293 cells (a HEK293 cell derivative, T-REx) and all clone/subcolonies  
553 including G11 clone cells that constitutively expressed His-tag hBCNT/CFDP1 [15]  
554 were routinely maintained in DMEM-GlutaMAX-1 (DMEM), which contained 10%  
555 Fetal calf serum, 50 µg/mL gentamicin, and with or without G418 (0.5 mg/mL) in 5%  
556 CO<sub>2</sub> incubator. For subculturing, the medium was aspirated completely, and the cell  
557 layers (2 ml culture on 35-mm dish) were incubated with 0.75 mL accutase for 5 min at

558 room temperature. Then, they were homogenized by pipetting using a 1000- $\mu$ L pipet  
559 tip, and 40-60  $\mu$ L of the suspension was directly plated on the dish preincubated with  
560 the 2 mL culture medium for at least 30 min, and G418 was added the next day when  
561 needed. For transfection or preparation of cellular protein extract, the cell layers (5 mL  
562 culture on 60-mm dish) were washed with 5 mL prewarmed Hepes buffered saline  
563 (HBS, [10 mM Hepes-NaOH, pH 7.5, 150 mM NaCl], treated with 1.5 mL accutase,  
564 homogenized as described above, and then 1 mL medium was added. The cell  
565 suspension was transferred to a 15-mL tube, and the dish was washed with another  
566 1-mL medium followed by combining the suspension within a total 10 min (total ~2.5  
567 mL). After taking out 20  $\mu$ L to estimate the cell number with a disposable  
568 Hemocytometer (Watson Bio Lab) , the suspension was centrifuged (Sakuma Model  
569 RSL-IV; 1, 000 rpm, 1 min, room temperature) and resuspended in the culture medium  
570 for further study. TrypLE Express was also used in the earlier stage of the study in  
571 isolation of T-Rex-derived colonies that constitutively expressed Flag-MCS or  
572 Flag-tagged mBcnt (see below).

573

574 **ES cell culture**

575 Cfdp1-K1 and vdR2-4 cells were obtained from Japanese Collection of Research  
576 Bioresources (JCRB) Cell Bank and grown in ESGRO Complete Clonal Grade Medium  
577 plus GSK3 $\beta$  Inhibitor (50  $\mu$ l/100 mL) supplemented with gentamicin (50  $\mu$ g/mL) in a  
578 35-mm dish that was precoated by incubation with recombinant human Laminin  
579 (iMatrix-511) at a final concentration of 5  $\mu$ g/mL in PBS for either 2 h at room  
580 temperature or 1 h at 37 °C. For subculturing, the medium was aspirated completely,  
581 and the cell layers were washed with 2 mL of prewarmed HBS and incubated  
582 with 0.75 mL accutase at room temperature. After 5 min, the cell layer was  
583 homogenized by pipetting using a 1000- $\mu$ L pipet tip, and 1-mL DMEM containing  
584 0.1% polyvinyl alcohol (DMEM-PVA) was added. The suspension was then transferred  
585 into a 15-mL tube and the dish was washed with another 1 mL of DMEM-PVA and the  
586 suspension was combined (total ~2.7 mL) within a total of 10 min. After taking out 20  
587  $\mu$ l for counting the cell number, the suspension was centrifuged (700 rpm, 3 min, room  
588 temperature) and resuspended in the new medium and seeded at the density of ~ 2.5 x  
589 10<sup>5</sup> cells per 35-mm dish. For the preparation of protein extract and total RNA, the cell

590 suspension obtained above were twice washed with chilled HBS, dispensed at  $\sim 1 \times 10^6$   
591 cells per 1.5-mL tube, and centrifuged (100 x g, 5 min, 4°C). After removing the buffer  
592 completely, the pelleted cells were softly vortexed, snap-frozen in liquid N<sub>2</sub>, and  
593 stocked at -80 °C until use.

594

### 595 **Generation of T-REx colonies expressing Flag-mBcnt**

596 T-REx cells ( $\sim 2 \times 10^6$  per 100-mm dish in 10 mL medium) were cultured for 20 h,  
597 and each 5 µg of pcDNA3.1 plasmid carrying Flag-MCS or Flag-*Bam*H1-mBcnt cDNA  
598 was added in the culture using Lipofectamine 3000 (5 µL in 250 µL Opti-MEM)  
599 according to the manufacturer protocol. Just before transfection, each 5 mL medium  
600 was once removed, transfected, and the medium that had been saved was back to the  
601 culture 4-6 h after transfection. After culturing for a total of 44-48 h, each cell layer was  
602 washed with 10 mL prewarmed HBS and treated with 1.5 mL of TrypLE Express for 10  
603 min at 37 °C, harvested using 1 mL of medium in a 15-mL tube, centrifuged and  
604 resuspended in a 1-mL medium.

605 The number of each cultured cell was counted, and  $\sim 60$  cells in 50 µL were seeded in a

606 48-well plate preincubated with 150- $\mu$ L medium. After 4 hours, G418 was added to a  
607 final concentration of 0.75 mg/mL. Colonies growing in 48-well plates were  
608 sequentially expanded to 12-well plates (on day 15 after media change twice) and  
609 35-mm dishes (on day 21 after media change twice). Each colonies was then maintained  
610 in the presence of 0.5 mg / mL G418.

611

## 612 **Protein extracts of T-REx cells and their colonies**

613 After washing with chilled HBS (10 mL/100-mm dish) followed by removing the  
614 buffer completely using a piece of filter paper, the cells were homogenized with a cell  
615 scraper (17-mm width) in 0.5 mL lysis buffer [20 mM Hepes-NaOH, pH 7.5, 150 mM  
616 NaCl, 1 mM 2-mercaptoethanol, designated L\_buffer] supplemented with both  
617 inhibitors of proteinases and phosphatases. The homogenate was transferred into a  
618 1.5-mL tube, sonicated by a Bioruptor (BM Equipment) in an ice-water bath (10-s  
619 pulses repeated 15 times at 10-s intervals) and centrifuged (25,000 x g, 30 min, 4 °C)  
620 using a centrifuge (Kubota 3780, rotor AF-2536A). After taking out five  $\mu$ L for  
621 measurement of protein concentration, the supernatants were aliquoted, snap-frozen in

622 liquid nitrogen, and stored at -80 °C until use. On the other hand, the pellets were  
623 dissolved in 50- $\mu$ L lysis buffer containing SDS [1%SDS, 1 mM EDTA in 10-mM  
624 Hepes-NaOH, pH 7.5, designated LS\_buffer], sonicated (3 x 10-s pulses at 10-s  
625 intervals) and centrifuged (10,000 x g, 1 min, 4°C) . After taking out 5  $\mu$ l for  
626 measurement of protein concentration, the sample was boiled in SDS/PAGE sample  
627 buffer.

628

## 629 **Isolation of F-mBcnt by anti-Flag Ab-conjugated agarose** 630 **beads**

631 The frozen supernatant of E3 colony was thawed, and Nonidet P-40 (NP-40) was  
632 added to a final concentration of 0.05%. After sonication for 30 s in the ice-water bath  
633 (3 x 10-s pulses at 10-s intervals) followed by centrifuging at 10, 000 x g for 1 min at  
634 4 °C, the sup (1 mL of 1.2 mg) was mixed with anti-Flag-tag agarose beads (20  $\mu$ L  
635 settled volume) in a 1.5-mL siliconized tube and incubated in a rotary shaker for 2 h at  
636 4 °C. The mixture was centrifuged for 30 s using a swing type centrifuge (Swing Man,  
637 Type ATT-101), and the supernatant was saved as the unbound fraction. The pellet was



638 suspended in 100- $\mu$ L of L\_buffer containing 0.05% NP-40 plus inhibitors and  
639 transferred to a spin column (0.8 mL size) using a 200- $\mu$ L wide-bore tip, and the tube  
640 was once more washed with 100  $\mu$ L of L\_buffer plus NP-40, and the suspension was  
641 recovered to the spin column. The through-flow fraction obtained by centrifugation was  
642 stocked as the first wash fraction. The agarose in the column was washed twice with the  
643 same buffer, followed by being washed once more with HBS, and then the bound  
644 proteins were eluted with 50  $\mu$ L of Flag (DYKDDDK) peptide (150  $\mu$ g in HBS) by  
645 incubation at 4  $^{\circ}$ C for 30 min (Eluate #1) and another 5 min (Eluate #2), sequentially.  
646 The agarose in a column was further treated with 50  $\mu$ L of glycine-HCl (50 mM, pH  
647 2.5), and its eluate and the agarose in the column were immediately neutralized with 2  
648 M Tris. Finally, 50  $\mu$ L of 1 x SDS/PAGE sample buffer was added to the column,  
649 vortexed, and boiled for 5 min. All of the fractionated samples except the fraction eluted  
650 with SDS/PAGE sample buffer were boiled in 1 x SDS/PAGE sample buffer by mixing  
651 with 4 x SDS/PAGE buffer. Each five  $\mu$ L (3.75  $\mu$ L of the net eluate) were separated on  
652 1.25 % SDA/PAGE and followed by western blotting analysis using anti-Flag Ab. For  
653 LC-MS/MS analysis, Eluates #1 and #2 described above (each  $\sim$ 40  $\mu$ L) were

654 concentrated with acetone according to the protocol  
655 (<http://tools.thermofisher.com/content/sfs/brochures/TR0049-Acetone-precipitation.pdf>). The  
656 dry pellet was once dissolved in 6  $\mu$ L of 10-fold diluted LS\_buffer, and two  $\mu$ L of 4  $\times$   
657 SDS/PAGE sample buffer was added followed by boiling for 3 minutes. After  
658 separating the sample for 10 minutes longer than usual on 12.5% gel SDS/PAGE, the  
659 gel was fixed with 50% MeOH-10% acetic acid solution for 20 minutes, stained with  
660 0.25% CBB for 10 minutes, and then de-stained in 10% MeOH-7% acetic acid solution.

661

## 662 **Protein extracts from mouse and rat brain**

663 Cerebrum and cerebral cortices were dissected from mice (P0 of C57BL/6J, male)  
664 and rats (P0-P56 of Wistar rat, male) after euthanasia under anesthesia, respectively.  
665 These isolated samples were snap-frozen in liquid N<sub>2</sub> and stored at -80 °C until use.  
666 Frozen samples were crushed with a hammer on dry ice and immediately transferred to  
667 a glass-Teflon homogenizer with 1 mL of LS\_buffer per 100 mg of samples. Then,  
668 tissues were homogenized at 600 rpm using a digital homogenizer and boiled for 5 min.  
669 These homogenates were sonicated (12 x 10-s pulses at 20-s interval) and centrifuged

670 (28,000 x g, 30 min, 20 °C). In the case of a mouse embryo on day around 17, a frozen  
671 piece (~40 mg) was wrapped with aluminum foil, crushed with pliers with the help of  
672 liquid nitrogen, transferred to a 1.5-mL BioMasher, and soaked in chilled 200 µL of  
673 LS\_buffer. Then, the tissues were homogenized in ice, boiled for 5 min, sonicated for  
674 2.5 min (15 x 10-s pulses at 10-s intervals), and centrifuged (15,000 x g, 10 min, 20 °C).  
675 The supernatants were used for western blot analysis. Protein concentrations in the  
676 supernatants were determined using a Bicinchoninic Acid (BCA) protein assay kit with  
677 bovine serum albumin as a standard.

678

### 679 **Enrichment of bovine Bcnt/Cfdp1 by Phos-tag agarose**

680 Bovine placenta (from Holstein Day 116) is a gift from Dr. Kazuyuki Hashizume  
681 (Iwate University, Morioka) and was stored in liquid nitrogen until use. Each piece (~30  
682 mg) was further subdivided with a razor blade and extracted in two ways: one for the  
683 whole extract preparation and the other for the concentration of Bcnt/Cfdp1 content.  
684 The minced pieces were placed in 1.5 mL of BioMasher, soaked in cold 200 µL of  
685 L\_buffer and homogenized, and then 10 µl of 20% SDS was mixed, followed by boiling

686 for 5 minutes. The extract was sonicated for 2.5 minutes (15 x 10-s pulses at 10-s  
687 intervals), centrifuged ( $15,000 \times g$ , 10 minutes, 22 °C.), and the supernatant was used as  
688 a whole extract. For enrichment of Bcnt/Cfdp1, the fined tissue piece in the 1.5-mL  
689 BioMasher was homogenized in 100  $\mu$ L of chilled RIPA buffer [20 mM Tris-HCl, pH  
690 7.5, 150 mM NaCl, 0.5% sodium deoxycholate, 1% NP-40, 1 mM EDTA] plus both  
691 inhibitors of proteinases/phosphatases. After transferring the homogenate into a new  
692 1.5-mL tube, the homogenizer was washed with another 100  $\mu$ L of RIPA buffer, and  
693 the solution was combined and centrifuged ( $15,000 \times g$ , 10 min, 4 °C). After taking out  
694 5  $\mu$ L for measurement of protein concentration, the supernatant was aliquoted,  
695 snap-frozen in liquid N<sub>2</sub> and stored in -80 °C until use (total 1.4 mg protein). After  
696 dilution of the supernatant with RIPA buffer, 100  $\mu$ L (200  $\mu$ g) was enriched by  
697 Phos-tag agarose (100  $\mu$ L settled volume in a spin column, 0.8 mL size) according to  
698 the manufactured protocol with the following modification; use of a swing-type  
699 centrifuge (Swing Man, Type ATT-101) and softly tapping the spin column during  
700 washing (200  $\mu$ L, three times) and elution (100  $\mu$ L per tube three times). Each eluate  
701 was precipitated with TCA at a final concentration of 20% and washed twice with 50

702  $\mu\text{L}$  of acetone according to the protocol  
703 ([http://www.its.caltech.edu/~bjorker/TCA\\_ppt\\_protocol.pdf](http://www.its.caltech.edu/~bjorker/TCA_ppt_protocol.pdf)). After heating at 95 °C, 50  
704  $\mu\text{L}$  of SDS/PAGE sample buffer was added and solubilized by a mixer (Tomy MT-360)  
705 for 30 min at room temperature. For larger preparation, the above 700  $\mu\text{g}$  of the extract  
706 was diluted to 350  $\mu\text{L}$  with RIPA buffer, applied to a 350- $\mu\text{L}$  settled volume of  
707 Phos-tag agarose in a spin column. After rinsing with 0.5 ml of washing buffer three  
708 times, the bound proteins were eluted with 0.5 and 0.45 mL of elution buffer  
709 sequentially into one tube, as described above. After precipitation with TCA, the pellets  
710 were mixed with 50  $\mu\text{L}$  of LS\_buffer for one hour. The total recovered protein was 112  
711  $\mu\text{g}$ , with a yield of 16 %. On the other hand, to estimate the approximate Bcnt/Cfdp1  
712 content in the pellet ( $\sim 20$   $\mu\text{L}$ ) of the above centrifugation (15,000 x g, 10 min, 4°C), 6.7  
713  $\mu\text{L}$  of 4 x SDS/PAGE sample buffer was added, mixed vigorously, boiled for 5 min, and  
714 sonicated for 2.5 min (15 x 10-s pulsed at 10-s intervals).

715

716 **Immunoblotting**

717 Procedures of SDS/PAGE of 12.5% or 15% gel and blotting onto membranes  
718 were mostly the same as previously described [15, 17]. The blotted PVDF membrane  
719 was blocked in 5% skim milk in TBT buffer [10 mM Tris-HCl, pH 7.6, 150 mM NaCl,  
720 0.1 % Tween 20] for 2 h at room temperature or overnight at 4 °C. The first Ab was  
721 incubated for 2 h at room temperature or overnight at 4 °C and the second Ab was  
722 treated for one h at room temperature. All immunoreactivity was visualized by  
723 chemiluminescent using horseradish peroxidase (HRP)-conjugated secondary antibodies  
724 that are listed in the S5 Table. Their image was detected by a scanner (GeneGenome,  
725 Syngene BioImaging) using ImmunoSTAR Zeta or LD as a substrate. For re-probing,  
726 the bound antibodies on the used membrane were stripped by incubation of the filters in  
727 a solution of 62.5 mM Tris-HCl (pH 6.8), 2% SDS, and 100 mM 2-mercaptoethanol  
728 with stirring for 30 min at ~60 °C on hot block, followed by washing three times with  
729 TBT buffer.

730

### 731 **Mass spectroscopy analysis**

732 The upper and lower bands of a doublet band that were detected by CBB staining

733 were cut out from the gel and digested with API, AspN, and chymotrypsin, and each  
734 digest was analyzed by nano-LC-MS/MS using a Q Exactive mass spectrometer as  
735 described previously [15]. The quantification of peptides derived from the upper and  
736 lower bands was carried out using a label-free quantification method using Proteome  
737 Discoverer Ver 2.2.0.388 (Thermo Fisher Scientific).

738

### 739 **Isolation of total RNA**

740 The frozen ES cells were homogenized with Trizol reagent, and total RNAs were  
741 purified using PureLink RNA Mini kit according to the manufacturer protocol [17]. The  
742 purified total RNAs were treated with TURBO DNase to eliminate contaminating  
743 genomic DNA, extracted with phenol/chloroform/isoamyl alcohol (pH 5.2), and  
744 re-purified using RNA Clean & Concentrator -25 kit. The concentration of the total  
745 RNAs was determined by the absorbance at 260 and 280 nm using NanoDrop One  
746 (Thermo Fisher Scientific), and the quality was estimated using a 2100 Bioanalyzer  
747 (Agilent). Two RNAs with the high quality shown below were subjected to RNA  
748 sequencing (Macrogen Japan Corp., Kyoto).

RNA source	Concentration (ng/ $\mu$ L)	A260/A280	RIN
Cfdp1-K1 (Bcnt/Cfdp1 Mutant)	454.6	2.07	9.9
vdR2-4 (Wild type)	366.8	2.03	9.6~9.9

749

750

## 751 **Reverse transcription-PCR and plasmid construction**

752 cDNAs were synthesized by Superscript III SuperMix according to the  
753 manufacturer protocol using oligo-(dT) 20 primer from purified total RNAs of  
754 Cfdp1-K1, vdR2-4 cells, and whole mouse brain of a P56 C57BL/6J male as previously  
755 described [17] . The full-length ORF of *mBcnt* or the fragment of *mBcnt* exons 1-5  
756 fused with *hygromycin phosphotransferase* were amplified from each cDNA (1 ng as a  
757 total RNA) by PCR using KAPA HiFi HotStart DNA polymerase under the following  
758 cycling conditions: denaturation at 95 °C for 3 min, followed by 35 cycles of 98 °C for  
759 10 sec, 68 °C for 15 sec, and 72 °C for 90 sec. The primer sequences are listed in S6  
760 Table. After confirmation of their amplicon size by 0.8% Tris-Acetate EDTA agarose  
761 gel electrophoresis and purification by Wizard SV Gel and PCR Clean-Up System



762 (Promega), the sequences of their ORFs were confirmed using BigDye Terminator V3.1  
763 Cycle Sequencing Kit (Thermo Fisher Scientific). For the construction of Flag-mBent  
764 expression plasmid, the PCR product was inserted into a mammalian expression vector,  
765 Flag-MCS-pcDNA3.1 (Accession No. LC311018), using restriction enzymes *Bam* HI  
766 and *Xho* I as previously described [17].

767

## 768 **Transcriptome analysis**

769 The following is from a report of HN00101712 (Macrogen Corp Japan, S1  
770 Appendix). The two cDNA libraries from RNAs of Cfdp1-K1 or vdR2-4 cells were  
771 prepared using the TruSeq Stranded mRNA LT Sample Prep Kit (Illumina). Their  
772 sequences were obtained using NovaSeq 6000 S4 Reagent Kit by a Nova Sequencing  
773 system (S1 Appendix, S2 Table). Paired-end reads (read length 101) were mapped to a  
774 mouse reference genome (UCSC GRCm38.p4/mm10, annotation RefSeq\_2017\_06\_12).  
775 After trimming, 98.81% were mapped on 45,262,214 cleaned reads from Cfdp1-K1  
776 RNA, while 99.09 % were mapped on 52,245,252 cleaned reads from vdR2-4 RNA.

777

## 778 **Acknowledgments**

779       We wish to thank Drs. Kyoji Horie and Eiji Kinoshita for providing technical  
780 suggestions and useful discussions on ES cell culture and Phos-tag agarose handling,  
781 respectively. We thank Drs. Kazuyoshi Hashizume and Takeharu Masaki for giving us  
782 bovine tissues and *Achromobacter* protease I, respectively, Dr. Wakako Kobayashi for  
783 sharing the interest in generating Bcnt/Cfdp1 knockout cells, and Dr. Sang Wan Kim for  
784 conducting the transcriptome analysis. We are grateful to Drs. Salvador Eugenio Caoili,  
785 Christopher A. MacRaid, and Brian McWilliams for their particularly useful  
786 discussions and opinions. We also thank Drs. Ed Luk, Takashi Yasuda for discussions  
787 on the chromatin remodeling complex and on repair of damaged DNA, respectively.  
788 We were indebted to Professor Hiromi Nochi for her encouragement.

789

## 790 **References**

- 791       1. Messina G, Celauro E, Atterato MT, Giordano E, Iwashita S, Dimitri P.  
792       The Bucentaur (BCNT) protein family: a long-neglected class of  
793       essential proteins required for chromatin/chromosome organization and

- 794 function. Chromosoma. 2015; 124(2):153-62. doi:  
795 10.1007/s00412-014-0503-8
- 796 2. Krogan NJ, Keogh MC, Datta N, Sawa C, Ryan OW, Ding H, et al. A  
797 Snf2 family ATPase complex required for recruitment of the histone  
798 H2A variant Htz1. Mol Cell. 2003; 12(6):1565-76.
- 799 3. Mizuguchi G, Shen X, Landry J, Wu WH, Sen S, Wu C. ATP-driven  
800 exchange of histone H2AZ variant catalyzed by SWR1 chromatin  
801 remodeling complex. Science. 2004; 303(5656):343-8.
- 802 4. Nguyen VQ, Ranjan A, Stengel F, Wei D, Aebersold R, Wu C, et al.  
803 Molecular Architecture of the ATP-Dependent Chromatin-Remodeling  
804 Complex SWR1. <https://doi.org/10.1016/j.cell.2013.08.018>.
- 805 5. Wu WH, Alami S, Luk E, Wu CH, Sen S, Mizuguchi G, et al. Swc2 is a  
806 widely conserved H2AZ-binding module essential for ATP-dependent  
807 histone exchange. Nat Struct Mol Biol. 2005; 12 (12):1064-71.
- 808 6. Tramantano M, Sun L, Au C, Labuz D, Liu Z, Chou M, et al.  
809 Constitutive turnover of histone H2A.Z at yeast promoters requires the

- 810 preinitiation complex. *Elife*. 2016; 5. pii: e14243. doi:  
811 10.7554/eLife.14243.
- 812 7. Lin CL, Chaban Y, Rees DM, McCormack EA, Ocloo L, Wigley DB.  
813 Functional characterization and architecture of recombinant yeast SWR1  
814 histone exchange complex. *Nucleic Acids Res*. 2017; 45(12): 7249-7260.  
815 doi: 10.1093/nar/gkx414.
- 816 8. Morillo-Huesca M, Clemente-Ruiz M, Andújar E, Prado F. The SWR1  
817 histone replacement complex causes genetic instability and genome-wide  
818 transcription misregulation in the absence of H2A.Z. *PLoS One*. 2010;  
819 5(8): e12143. doi: 10.1371/journal.pone.0012143.
- 820 9. Sun L, Luk E. Dual function of Swc5 in SWR remodeling ATPase  
821 activation and histone H2A eviction. *Nucleic Acids Res*. 2017; 45(17):  
822 9931-9946. doi: 10.1093/nar/gkx589.
- 823 10. Messina G, Damia E, Fanti L, Attarrato MT, Celauro E, Mariotti FR, et  
824 al. *Yeti*, an essential *Drosophila melanogaster* gene, encodes a protein  
825 required for chromatin organization. *J Cell Sci* 2014; 127: 2577-2588;

- 826 doi: 10.1242/jcs.150243.
- 827 11. Ohta S, Bukowski-Wills JC, Sanchez-Pulido L, Alves Fde L, Wood L,  
828 Chen ZA, et al. The protein composition of mitotic chromosomes  
829 determined using multiclassifier combinatorial proteomics. *Cell*. 2010;  
830 142(5): 810-21. doi: 10.1016/j.cell.2010.07.047.
- 831 12. Morozov VM, Giovinazzi S, Ishov AM. CENP-B protects centromere  
832 chromatin integrity by facilitating histone deposition via the  
833 H3.3-specific Daxx. *Epigenetics Chromatin*. (2017) 10(1):63. doi:  
834 10.1186/s13072-017-0164-y.
- 835 13. Clément-Ziza M, Marsellach FX, Codlin S, Papadakis MA, Reinhardt S,  
836 Rodríguez-López M, Martin S, Marguerat S, et al. Natural genetic  
837 variation impacts expression levels of coding, non-coding, and antisense  
838 transcripts in fission yeast. *Mol Syst Biol*. 2014;10: 764. doi:  
839 10.15252/msb.20145123.
- 840 14. Liu Y, Beyer A, Aebersold R. On the Dependency of Cellular Protein  
841 Levels on mRNA Abundance. *Cell*. 2016;165(3): 535-550. doi:

- 842                   10.1016/j.cell.2016.03.014.
- 843                   15. Iwashita S, Suzuki T, Yasuda T, Nakashima K, Sakamoto T, Kohno T, et  
844                   al. Mammalian Bcnt/Cfdp1, a potential epigenetic factor characterized  
845                   by an acidic stretch in the disordered N-terminal and Ser250  
846                   phosphorylation in the conserved C-terminal regions. Biosci Rep. 2015;  
847                   35(4). pii: e00228. doi: 10.1042/BSR20150111.
- 848                   16. Iwashita S, Osada N, Itoh T, Sezaki M, Oshima K, Hashimoto E, et al. A  
849                   transposable element-mediated gene divergence that directly produces a  
850                   novel type bovine Bcnt protein including the endonuclease domain of  
851                   RTE-1. Mol Biol Evol. 2003; 20(9):1556-63. doi:  
852                   10.1093/molbev/msg168
- 853                   17. Nakashima K, Iwashita S, Suzuki T, Katoh C, Kohno T, Kamei Y, et al.  
854                   A spatial similarity of stereochemical environments formed by amino  
855                   acid residues defines a common epitope between two non-homologous  
856                   proteins. Scientific Rep (in press).
- 857                   18. Horie K, Kokubu C, Yoshida J, Akagi K, Isotani A, Oshitani A, et al. A

- 858 homozygous mutant embryonic stem cell bank applicable for  
859 phenotype-driven genetic screening. Nat Methods. 2011; 8(12):  
860 1071-1077. doi: 10.1038/nmeth.1739.
- 861 19. Kinoshita-Kikuta E, Yamada A, Inoue C, Kinoshita E, Koike E. A novel  
862 phosphate-affinity bead with immobilized Phos-tag for separation and  
863 enrichment of phosphopeptides and phosphoproteins. OMICS 2011;1(1)  
864 157-169.
- 865 20. Passon DM, Lee M, Rackham O, Stanley WA, Sadowska A, Filipovska  
866 A, et al. Structure of the heterodimer of human NONO and paraspeckle  
867 protein component 1 and analysis of its role in subnuclear body  
868 formation. Proc Natl Acad Sci U S A. 2012;109(13):4846-50. doi:  
869 10.1073/pnas.1120792109.
- 870 21. Kobayashi W, Ozawa M. The epithelial-mesenchymal transition induced  
871 by transcription factor LEF-1 is independent of  $\beta$ -catenin. Biochem  
872 Biophys Rep. 2018; 15: 13-18. doi: 10.1016/j.bbrep.2018.06.003.

- 873           22. Iwashita S1, Ueno S, Nakashima K, Song SY, Ohshima K, Tanaka K, et  
874           al. A tandem gene duplication followed by recruitment of a  
875           retrotransposon created the paralogous bucentaur gene (bcntp97) in the  
876           ancestral ruminant. *Mol Biol Evol.* 2006; 23(4): 798-806. doi:  
877           10.1093/molbev/msj088
- 878           23. Iwashita S, Nakashima K, Sasaki M, Osada N, Song SY. Multiple  
879           duplication of the bucentaur gene family, which recruits the APE-like  
880           domain of retrotransposon: Identification of a novel homolog and  
881           distinct cellular expression. *Gene.* 2009;435(1-2):88-95. doi:  
882           10.1016/j.gene.2009.01.012.
- 883           24. Vanli G, Cuesta-Marban A, Widmann C. Evaluation and validation of  
884           commercial antibodies for the detection of Shb. *PLoS One.* 2017; 12(12):  
885           e0188311. doi: 10.1371/journal.pone.0188311.
- 886           25. Qi W, Davidson BA, Nguyen M, Lindstrom T, Grey RJ, Burnett R, et al.  
887           Validation of anti-glucocerebrosidase antibodies for western blot  
888           analysis on protein lysates of murine and human cells. *Biochem J.* 2019;



- 889 476(2): 261-274. doi: 10.1042/BCJ20180708.
- 890 26. MacRaild CA, Richards JS, Anders RF, Norton RS. Antibody  
891 Recognition of Disordered Antigens. *Structure*. 2016; 24(1): 148-157.  
892 doi: 10.1016/j.str.2015.10.028.
- 893 27. McIntush EW. Response: Antibody crossreactivity between the tumour  
894 suppressor PHLPP1 and the proto-oncogene  $\beta$ -catenin. *EMBO Rep*.  
895 2013; 14(6): 494-6. doi: 10.1038/embor.2013.68.
- 896 28. Uhlen M, Bandrowski A, Carr S, Edwards A, Ellenberg J, Lundberg E,  
897 et al. A proposal for validation of antibodies. *Nat Methods*. 2016; 13(10):  
898 823-7. doi: 10.1038/nmeth.3995.
- 899 29. Caoili SE, Expressing Redundancy among Linear-Epitope Sequence  
900 Data Based on Residue-Level Physicochemical Similarity in the Context  
901 of Antigenic Cross-Reaction. *Adv Bioinformatics*. 2016; 1276594. doi:  
902 10.1155/2016/1276594.
- 903 30. Dalkas GA, Rooman M. SEPIa, a knowledge-driven algorithm for  
904 predicting conformational B-cell epitopes from the amino acid

- 905 sequence. BMC Bioinformatics 2017;18(1):95. doi:  
906 10.1186/s12859-017-1528-9.
- 907 31. Piotrowska U, Adler G. Phosducin and monomeric  $\beta$ -actin have common  
908 epitope recognized by anti-phosducin antibodies. Immunol Lett.  
909 2010;134(1):62-68. doi: 10.1016/j.imlet.2010.08.010.
- 910 32. Forsström B, Axnäs BB, Stengele KP, Bühler J, Albert TJ, Richmond  
911 TA, et al. Proteome-wide epitope mapping of antibodies using  
912 ultra-dense peptide arrays. Mol Cell Proteomics. 2014; 13(6): 1585-97.  
913 doi: 10.1074/mcp.M113.033308.
- 914 33. Forsström B, Axnäs BB, Rockberg J, Danielsson H, Bohlin A, Uhlen M  
915 (2015) Dissecting antibodies with regards to linear and conformational  
916 epitopes. PLoS One 10 (3) :e0121673.
- 917 34. McLane MW, McCann U, Ricaurte G. Identifying the serotonin  
918 transporter signal in Western blot studies of the neurotoxic potential of  
919 MDMA and related drugs. Synapse. 2011; 65(12):1368-72. doi:  
920 10.1002/syn.20958.

- 921            35. Jank T, Bogdanović X, Wirth C, Haaf E, Spoerner M, Böhmer  
922            KE, et al. A bacterial toxin catalyzing tyrosine glycosylation of  
923            Rho and deamidation of Gq and Gi proteins. *Nat Struct Mol*  
924            *Biol.* 2013; 20(11):1273-80. doi: 10.1038/nsmb.2688.
- 925            36. Saykali B, Mathiah N, Nahaboo W, Racu ML, Hammou L, Defrance M,  
926            et al. Distinct mesoderm migration phenotypes in extra-embryonic and  
927            embryonic regions of the early mouse embryo. *Elife.* 2019;8. pii:  
928            e42434. doi: 10.7554/eLife.42434.

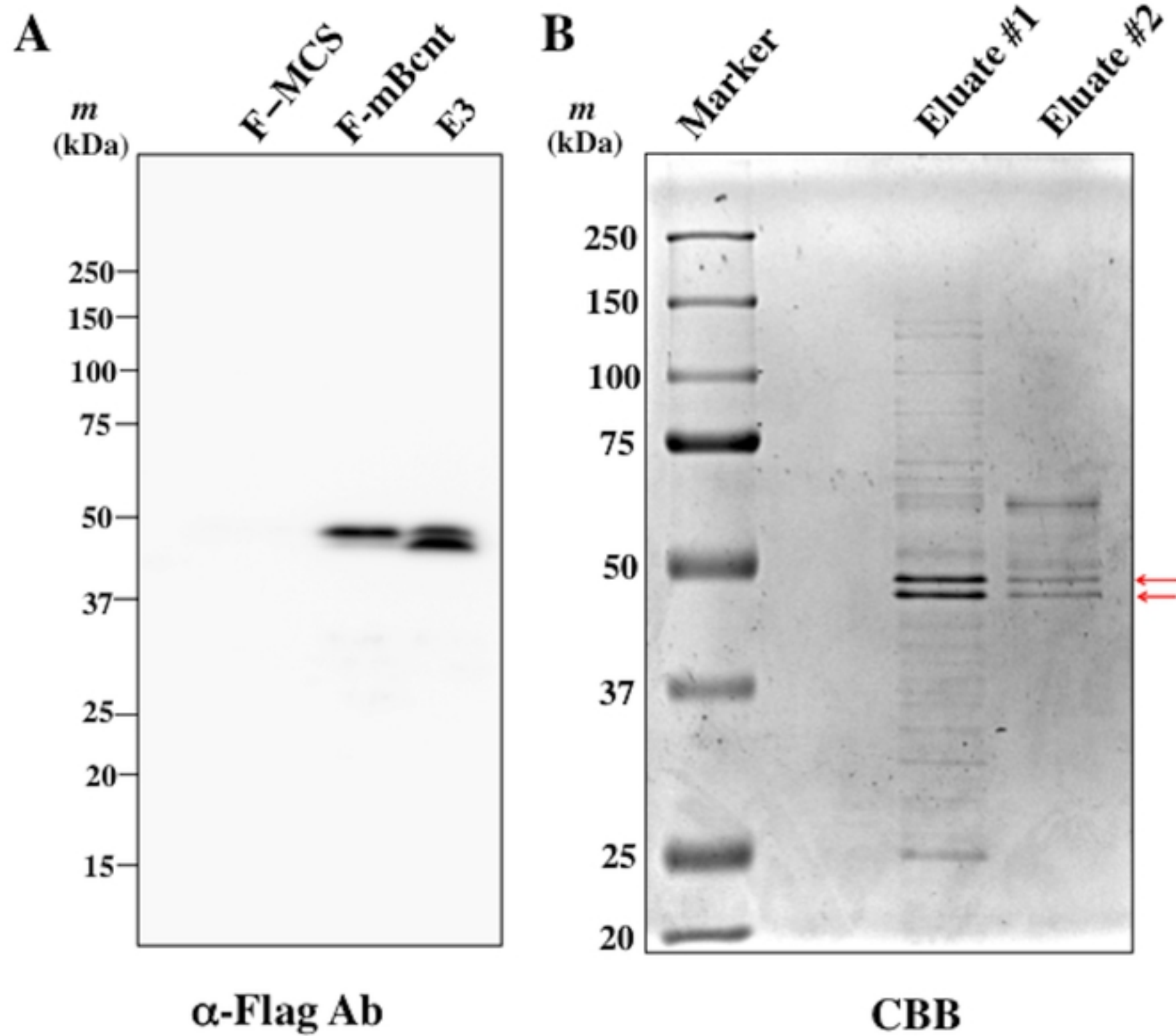
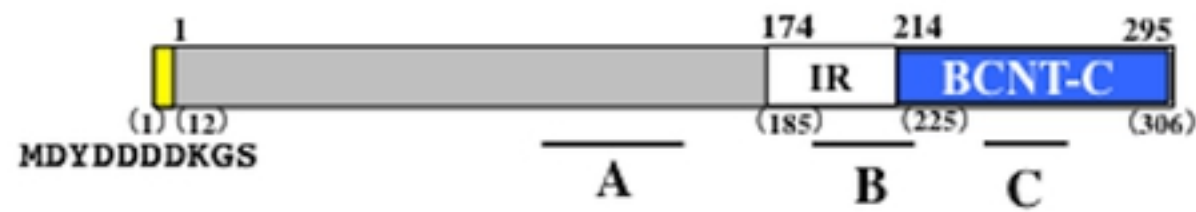


Fig 1.tif



Phosphorylated Fragments  
 Unphosphorylated Fragments

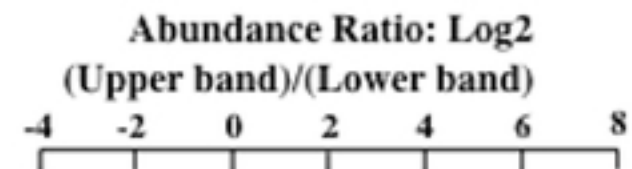


Fig 2.tif

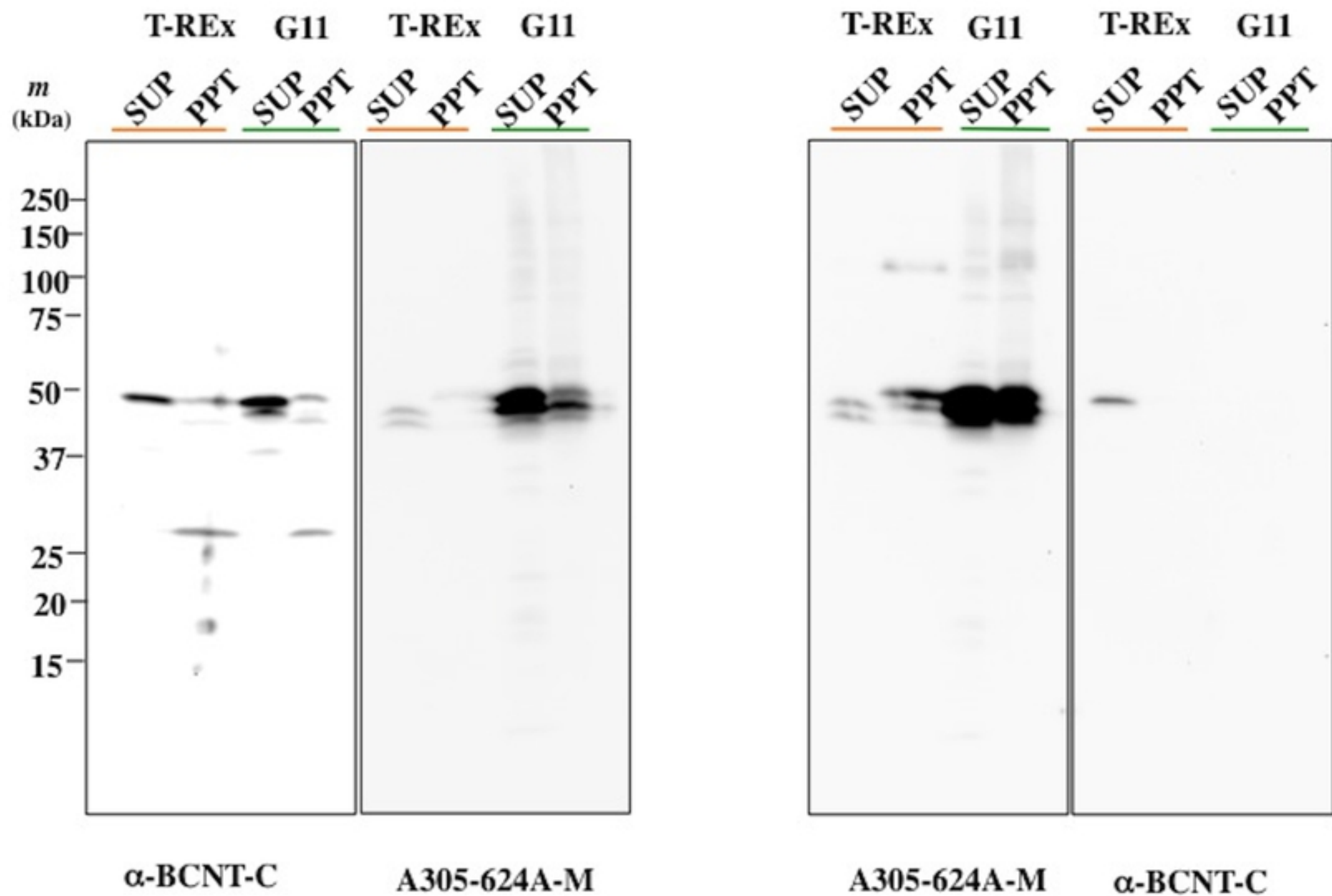


Fig 3.tif

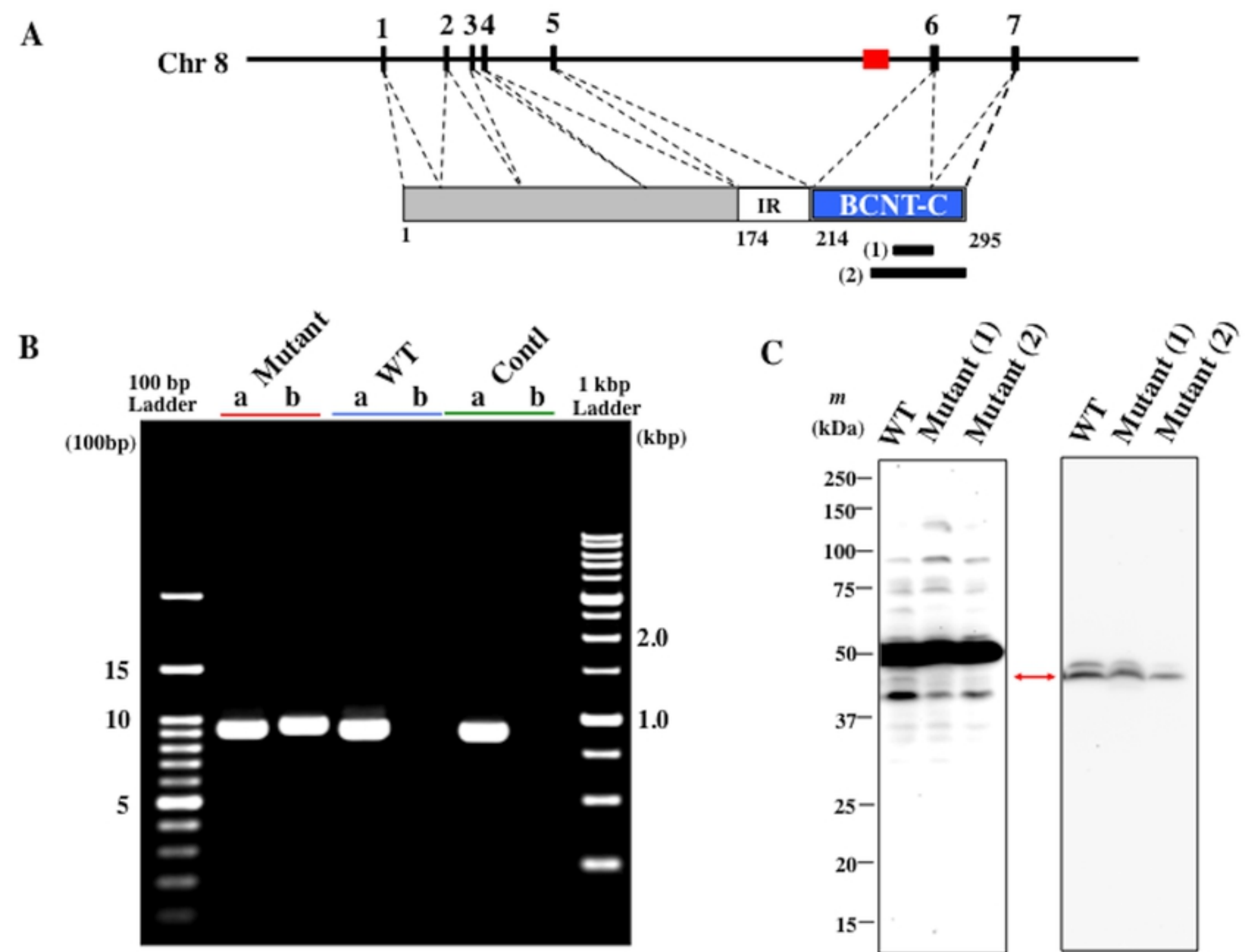


Fig 4.tif



Mouse  
 Rat  
 Bovine

41 GEEQAEKTKGKRRKAQ 56  
 GEEQAEKTKGKRRKAQ  
 GEE**ETQ**KTKG**TKR**KA**E**

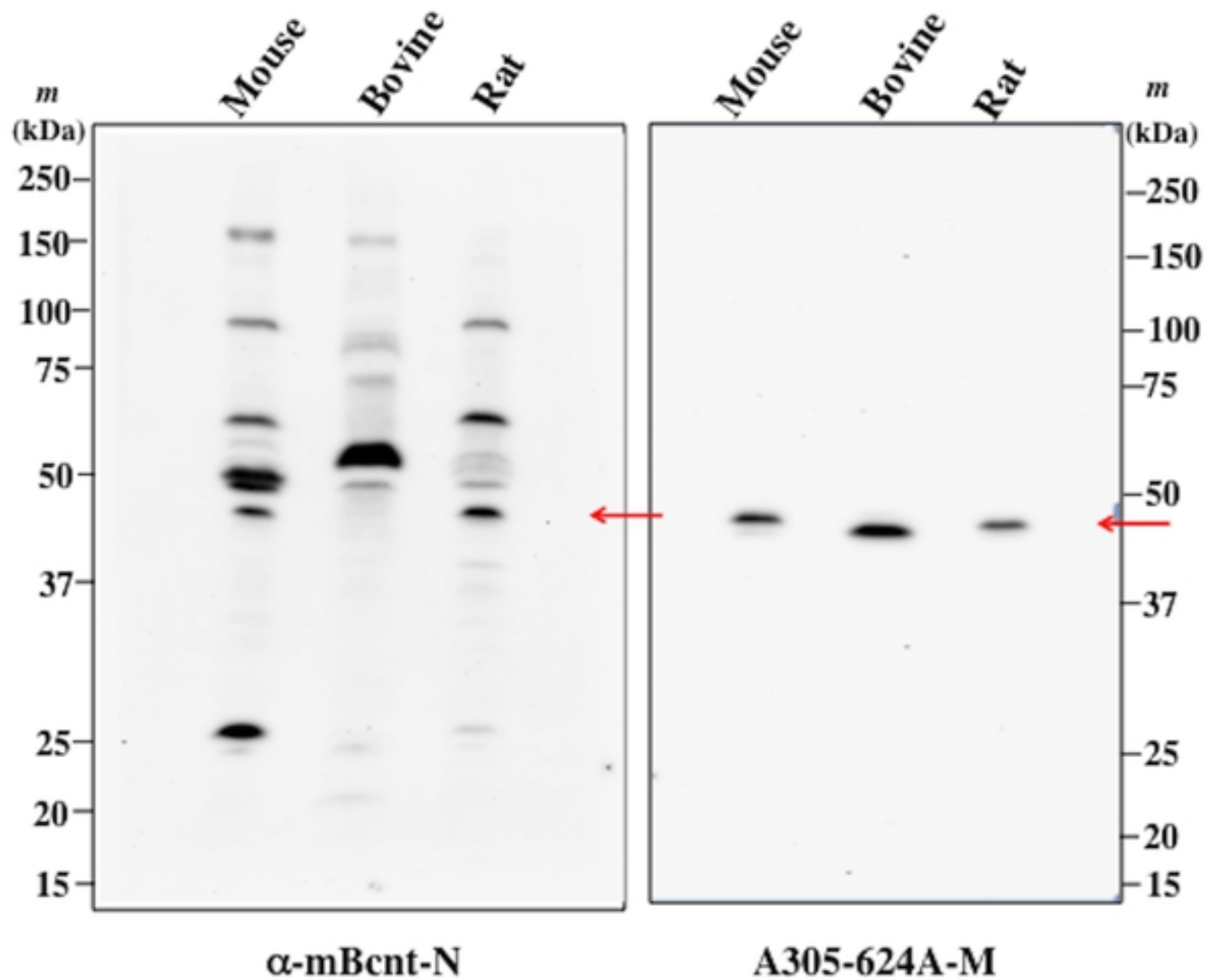


Fig 5.tif



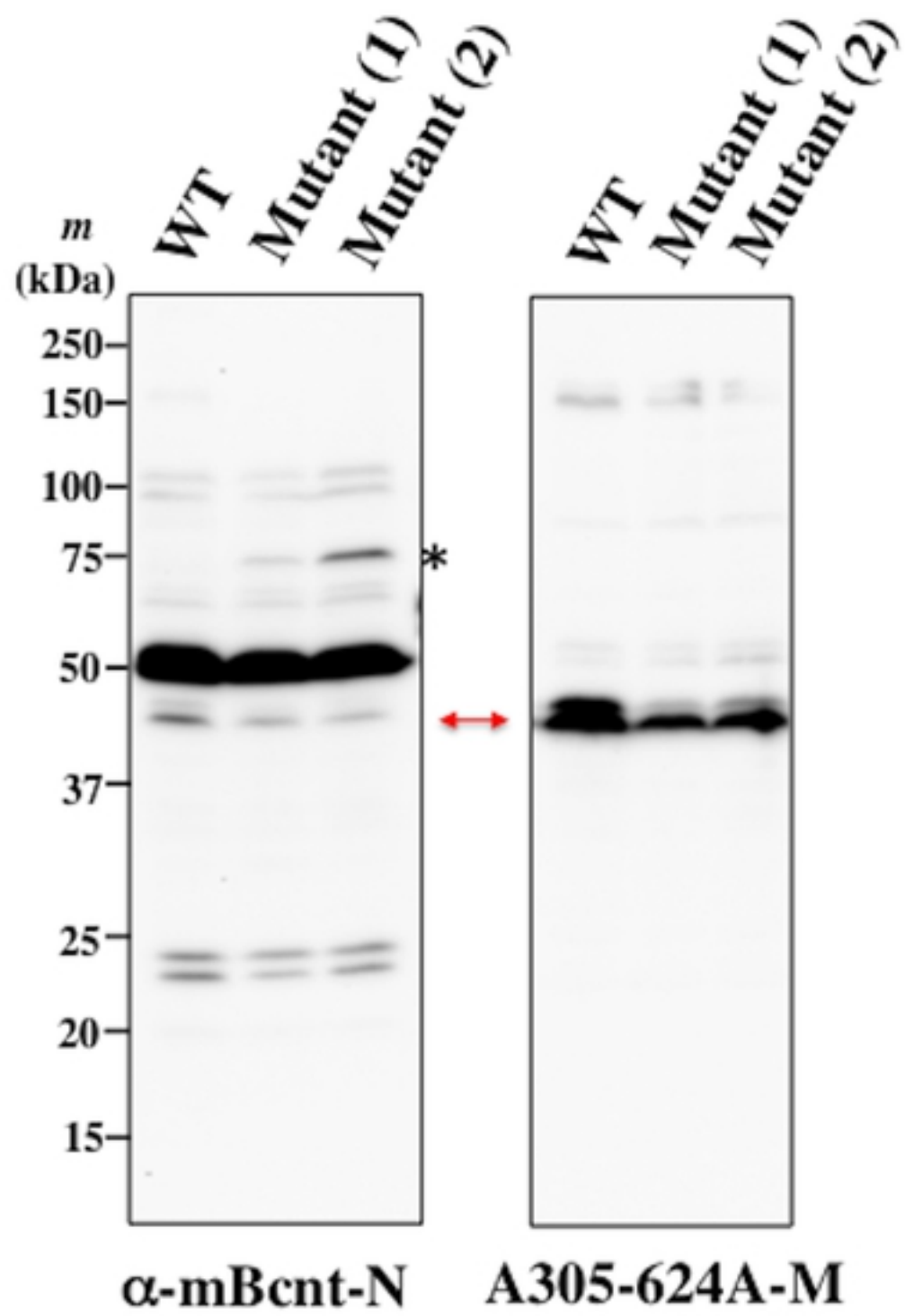


Fig 6.tif

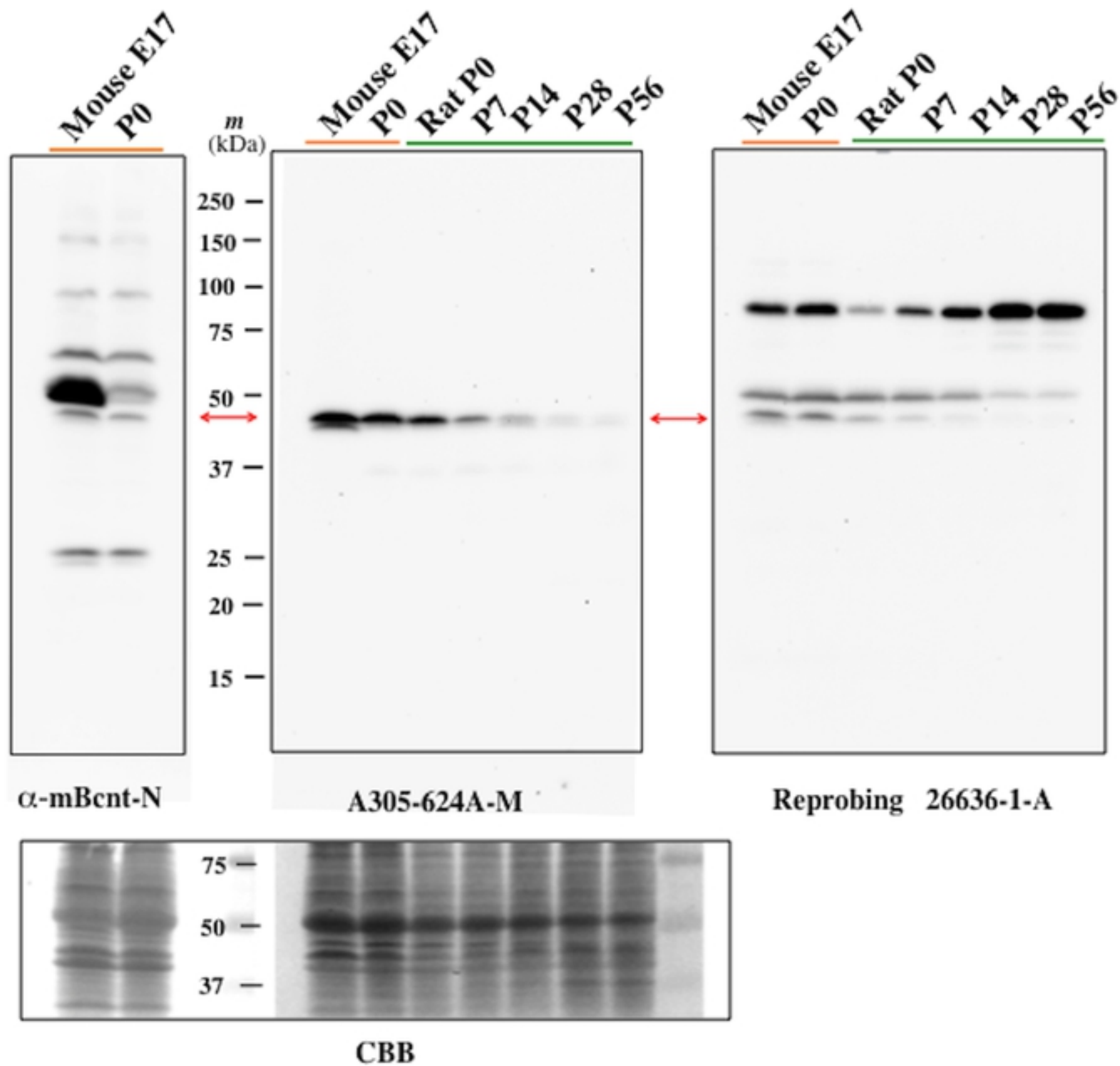


Fig 7.tif